Medicinal Chemistry Research
https://doi.org/10.1007/s00044-019-02498-z

MEDICINAL CHEMISTRY RESEARCH

ORIGINAL RESEARCH

Naphthoquinones isolated from *Eleutherine plicata* herb: in vitro antimalarial activity and molecular modeling to investigate their binding modes

Valdicley Vieira Vale[1] · Jorddy Neves Cruz[2] · Giselle Maria Rachid Viana[3] · Marinete Marins Póvoa[3] · Davi do Socorro Barros Brasil[1,2] · Maria Fani Dolabela[1]

Received: 15 October 2019 / Accepted: 30 December 2019

Abstract

Plasmodium falciparum is the cause of malaria and has become resistant to the drugs used to treat the disease. Therefore, the development for novel compounds with antimalarial activity has become urgent. Plant species, such as naphthoquinone-rich *Eleutherine plicata*, may provide novel substances that exhibit antimalarial activity and serve as an alternative for the treatment of this disease. From this plant species, ethanol extracts were obtained, fractionated, and the isolated substances eleutherin, and isoleutherin were characterized by nuclear magnetic resonance. There in vitro activity against *Plasmodium falciparum* was examined using the traditional Microtest method using the extract, fractions, and isolated molecules. Eleutherin and isoleutherin showed the best activity toward the parasite with IC_{50} values of 10.45 and 8.70 µg/mL, respectively. Characterization of the binding mode of the compounds with a target enzyme and identification of the molecular interactions were revealed via molecular docking results. Eleutherin and isoeleutherin interacted with highly conserved residues from the binding cavity of the cytochrome bc_1 complex, a protein found in mitochondria. Therefore, the eleutherin and isoeleutherin naphthoquinones showed antiplasmodial activity with a similar mechanism to that of atovaquone were able to interact with the cytochrome bc_1 complex, and showed promise for antimalarial treatments.

Keywords *Eleutherine plicata* · Naphthoquinones · Antimalarial activity · Molecular modeling

Introduction

Malaria is an infectious disease caused by six species of *Plasmodium: P. falciparum, P. vivax, P. malariae, P. ovale, P. knowlese*, and *P. cinomolgi*. All of them capable of infecting humans (Singh and Daneshvar 2013). The lifecycle of this disease involves two hosts: the first one is the human being and the other is the female *Anopheles* mosquito, which also act as a vector. In humans (vertebrate host), the asexual phase of the cycle occurs, with liver preerythrocytic schizogony and erythrocytic schizogony; in the mosquito, sporogony (sexual phase) is developed (Siciliano and Alano 2015).

Disease manifestation takes place after a period of plasmid incubation that varies according to each species. The clinical picture occurs when schizonts break the erythrocyte and release together with the merozoites, proinflammatory cytokines, which activate the immune system causing fever and chills. After fever, the patient might have sweating. In addition, the clinical picture may be accompanied by nausea, vomiting, headache, and muscle pain (Talapko et al. 2019). The symptoms cycle (fever-chills-sweating) appears several times with intervals that vary according to the *Plasmodium* species that infected the patient. For *P. falciparum*, *P. vivax*, and *P. ovale*, the cycle usually occurs at 3-day intervals; for *P. malariae*, every

Supplementary information The online version of this article (https://doi.org/10.1007/s00044-019-02498-z) contains supplementary material, which is available to authorized users.

✉ Maria Fani Dolabela
fanidolabela20@gmail.com

[1] Programa de Pós-Graduação em Inovação Farmacêutica, Instituto Ciências da Saúde, Universidade Federal do Pará, Belém, PA, Brazil

[2] Instituto de Tecnologia, Universidade Federal do Pará, Belém, PA, Brazil

[3] Instituto Evandro Chagas, Ananindeua, PA, Brazil

Published online: 18 January 2020

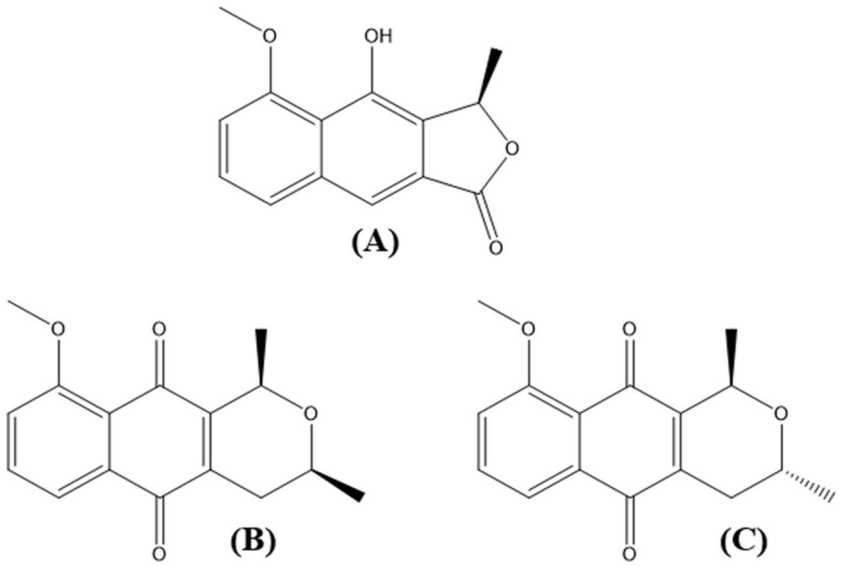

Fig. 1 Major substances isolated from *Eleutherine plicata*: **a** eleutherol, (**b**) eleutherin, and (**c**) isoeleutherin

4 days; and for *P. knowlese*, every 24 h (Phillips et al. 2017). In some cases, *P. falciparum* infection may evolve to severe malaria, which in addition to fever, may be accompanied by a syndrome with hypoglycemia, pulmonary edema, renal failure, metabolic acidosis, severe anemia, and cerebral malaria, which may progress to death (Geleta and Ketema 2016; Cowman et al. 2016).

In 2017, 219 million cases of malaria were recorded worldwide, two million more than in 2016, resulting in 435,000 deaths, of which 403,000 occurred on the African continent. In Africa, the most widespread Plasmodium is *P. falciparum*, which causes severe malaria (WHO 2018).

Malaria infection has become increasingly severe due to parasite resistance to drugs used in its pharmacological treatment (Wang et al. 2015). Due to this problem, the search for new antimalarial drugs is urgent, and natural compounds of plant origin can help in this search by providing unpublished substances or scaffolds that support drug design (Newman and Cragg 2016; Das et al. 2017).

Several antimalarial drugs have been discovered from natural products or are analogous to compounds of natural origin. For example, the alkaloid quinine, isolated from *Cinchona officinalis*, was one of the first natural compounds of plant origin with reported antimalarial activity. From these compounds, some antimalarial quinolines, such as chloroquine and mefloquine, were synthesized. Artemisinin-type compounds, such as artemisinin, obtained from *Artemisia annua*, and its synthetic analogs artesunate and artemether, are also used in malaria treatment, acting on the parasite erythrocytic cycle, as well as molecules belonging to quinoline class. Atovaquone, which belongs to the class of naphthoquinones, is one of the main drugs used in malaria treatment, being a structural analog of lapachol, which can be isolated from trees of Bignoniaceae family.

Plants of the genus *Eleutherine* (Iridaceae family) produce many naphthoquinone secondary metabolites. Some species of this genus include *Eleutherine plicata* herb. ex Klatt, *Eleutherine americana* (Aubl.) Merr. ex K. Heyne, and *Eleutherine palmifolia* (L.) Merr (Klotz et al. 2014).

The *Eleutherine plicata* herb species is popularly used for the treatment of malaria, gastric ulcers, amoeba infection, parasitic infection, dysenteries, diarrhea, bowel disorders, hemorrhoids, and menstrual disorders (Rahmatullah et al. 2012; Couto et al. 2016).

From the bulbs of this species, several naphthoquinones, naphthalene, anthraquinone, and terpene compounds have been isolated. Among the isolated products, the major constituents of the *Eleutherine plicata* extract include eleutherol, eleutherin, and isoleutherin (Fig. 1).

Although this herb species is popularly used for malaria treatment, the activity of the isolated compounds from *E. plicata* towards the causative agent of malaria remains unknown (Alves et al. 2003; Hong et al. 2008; Kusuma et al. 2010). Therefore, here for the first time the antimalarial activities of eleutherol, eleutherin, and isoleutherin isolated from *E. plicata* were determined. In addition, molecular modeling approaches were used to analyze the molecular binding mode of these compounds with the mitochondrial cytochrome bc_1 complex, as the mitochondria was the main organelle that suffered damage after treatment of *P. falciparum* with the isolated compounds. The choice of this target was based on the fact that another naphthoquinone and atovaquone, binds to this protein, resulting in the antimalarial effect.

Materials and methods

General experimental procedures

Nuclear magnetic resonance (NMR) spectra were measured using a Bruker Advance DPX 300 MHz NMR spectrometer (Karlsruhe, Germany). Precoating of thin layer chromatography plates was performed using silica gel 60 (MACHEREY-NAGELY, Germany). Chromatographic column was prepared using silica gel 60 (0.063–0.200 mm, 70–230 mesh, Merck, Germany). Hexane, dichloromethane, ethyl acetate, and methanol (Isofar, Brazil) were used as the mobile phase. Water was used in the high-performance liquid chromatography (HPLC) procedure (model 2695, PDA 2996, EUA), equipped with a RP-18 column (5 µm, 250 × 46 mm, LiChrospher, Merck, Germany).

Plant material and extraction procedure

E. plicata bulbs were collected from the municipality of Traquateua, PA, Brazil (Lat. 1.1436°, Long. 46.95511°) in the Amazon. The dried specimens were deposited at the Emílio Goeldi Paraense Museum (exemplary voucher: MG. 202631). Subsequently, the bulbs were washed and dried in a ventilated oven and ground using a knife mill.

The powder (0.5 kg) was macerated with ethanol (2 L, for 7 days), followed by concentration in a rotary evaporator to obtain an ethanol extract (42 g). Ethanol extract (7 g) was fractionated by solid–liquid chromatography using silica gel as the stationary phase of silica gel, eluting with increasing polarity solvents (hexane, dichloromethane, acetate methanol), thus obtaining four fractions: hexane (0.21 g), dichloromethane (0.65 g), ethyl acetate (1.10 g), and methanol (3.5 g).

The dichloromethane fraction was then refracted by preparative CCD obtaining four subfractions. Fraction S1 was identified later. Subfraction 2 (S2; 70 mg) was then refracted by column solid–liquid chromatography (235 × 10 mm silica gel; 230 × 400 mesh, 40–63 µm) eluted with dichloromethane, showing two isolated products identified by ^{1}H NMR.

Phytochemical study

The isolated substances were identified by ^{1}H NMR and compared with the literature data (Alves et al. 2019). Deuterated chloroform solvent was used for the NMR experiments.

The ethanol extract, fractions, and isolated substances were evaluated by high-performance liquid chromatography with a diode array detector (HPLC-DAD) and reverse column C-18 at 40 °C, 1 mL/min flow rate, and detection at 200–400 nm. As a mobile phase, a linear gradient of 20% (acetonitrile) and 80% (water) at 0 to 30 min ending with 80% (acetonitrile) and 20% (water) was (Paramapojn et al. 2008).

The spectroscopic evidence of isolated substances is in accordance with previous reports for eleutherin (Tewierik et al. 2006; Hara et al. 2011) and isoeleutherin (Gallo et al. 2010; Hara et al. 2011).

Eleutherin—^{1}H NMR 300 MHz ($CDCl_3$): δ 1.35 ppm (3H, d, $J = 6$ Hz, Me-11); δ 1.53 ppm (3H, d, $J = 6.6$ Hz, Me-1); δ 2.19 ppm (1H, dd, $J = 10.2$e 18.3 Hz, H-4ax); δ 2.74 ppm (1H, dt, $J = 13.2$e 18 Hz, H-4eq); δ 4.0 ppm (3H, s, OMe-9); δ 7.64 ppm (1H, t, $J = 8.1$ Hz, H-6); δ 7.73 ppm (1H, dd, $J = 1.2$; 7.8, H-7); δ 7.27 ppm (1H, d, $J = 8.4$, H-8) (Fig. S1).

Isoeleutherin—^{1}H NMR 300 MHz ($CDCl_3$): δ 1.35 ppm (3H, d, $J = 6$ Hz, Me-3); δ 1.53 ppm (3H, d, $J = 6.9$ Hz, Me-1); δ 2.23 ppm (1H, ddd, $J = 18.9$; 10.2; 1.8 Hz, H-4ax); δ 2.69 ppm (1H, dd, $J = 18.6$; 2.7 Hz, H-4eq); δ 4.0 ppm (3H, s, OMe-9); δ 3.99 ppm (1H, m, H-3); δ 5.01 ppm (1H, q, $J = 6.9$ Hz, H-1); δ 7.65 ppm (1H, t, $J = 7.8$ Hz, H-6); δ 7.74 ppm (1H, dd, $J = 7.5$; 0.9 Hz, H-7); δ 7.27 ppm (1H, dd, $J = 7.5$ Hz, H-8) (Fig. S2).

Eleutherol has been identified by co-injection into HPLC-DAD, with a standard (Guide Chem, 480-00-2, China).

In vitro antimalarial activity

For the biological assay, the methodology described by Rieckmann et al. (1978) and modified by Carvalho and Krettli (1991). A chloroquine sensitive *P. falciparum* clone (3D7) was used, synchronized using the sorbitol method (Lambros and Vanderberg 1979) followed by parasitemia adjustment to 0.5% and hematocrit to 5%. The samples and control was solubilized in methanol and serial dilutions were performed, finally obtaining a dosed plate with the samples at concentrations of 200, 100, 50, 25, 12.5, 6.25, and 3.125 µg/mL. The plates were incubated at 37 °C and 5% CO_2 atmosphere.

After 24 and 48 h, the supernatant was changed and new complete medium was added to the samples and controls. After 72 h, blood strains of red blood cell (3 µL) were fixed with methanol and stained with Giemsa. Each sample was tested in triplicate and three independent experiments were performed.

In each stained slide, for determination of parasitaemia, 5000 red blood cells were counted. Slide counting was performed in a blind experiment. The parasitaemia was determined as a percentage. The reduction index was determined from the negative control. The IC_{50} was determined from three independent experiments using the Graph Pad Prism 7.0 program by linear regression. The samples were classified as inactive ($IC_{50} > 100$ µg/mL), moderately

active (IC_{50} 100–10 µg/mL), active (IC_{50} < 10−1 µg/mL), or very active (IC_{50} < 1 µg/mL) (Dolabela et al. 2015b).

Molecular docking simulations

Eleutherin and isoeleutherin molecular structures were designed using GaussView 6 software (Dennington et al. 2016). The structures were optimized using density functional theory with the B3LYP hybrid functional and the 6-31G * basis set (Becke 1993). Structural optimization calculations were performed using Gaussian 16 (Frisch et al. 2016).

Prediction of the binding mode of eleutherin and isoeleutherin to the mitochondrial cytochrome bc_1 complex (cyt bc_1) was studied using Molegro Virtual Docker 5.5 (René Thomsen et al. 2006) with the MolDock score function at a grid resolution of 0.30 and the MolDock SE algorithm. The three-dimensional structure of cyt bc_1 protein was obtained from the protein data bank (PDB ID: 4PD4) (Birth et al. 2014a).

To validate the docking protocol, the crystallographic complex was re-docked. Redocking experiments with known complexes with inhibitors of similar conformational complexity are typically performed to evaluate the docking protocol, as previously suggested (Junior et al. 2019; Neves Cruz et al. 2019a; da Costa et al. 2019).

Results and discussion

Phytochemistry

E. plicata ethanol extract (7 g) was fractionated by silica gel packed chromatographic column and eluted with increasing polarity solvents to obtain four fractions: hexane (0.21 g, 0.3%), dichloromethane (0.65 g, 9.28%) ethyl acetate (1.1 g, 15.7%), and methanol (3.5 g, 50%). HPLC-DAD analyses of the fractions are shown in Fig. S3.

HPLC-DAD analysis of the ethanol extract (Fig. S3A) suggested the presence of high and medium polarity compounds. The moderately polar peaks at 16.4 and 16.8 min showed the same absorption profile with maxima at 247 and 270 nm. It is likely that they correspond to isomeric naphthoquinone as they contain the same chromophore, likely eleutherin, and isoeleutherin (Hong et al. 2008). The peak at 17.2 min showed maximum absorptions at 247, 315, and 363 nm, likely corresponding to naphthalene.

The dichloromethane fraction showed more intense peaks with retention times of between 16 and 17.9 min. The ultraviolet absorbances of at 218, 315, and 363 nm, corresponding to naphthalene chromophore previously mentioned (Fig. S3B). This fraction was chosen for fractionation because it contains higher content of substances of interest (eleutherin and isoeleutherin).

The ethyl acetate fraction (Fig. S3C) showed overlap of three peaks at 16.9 min with maximum ultraviolet absorbances at 247 and 270 nm. These spectra repeat at peak within 17.4 min, demonstrating that they may be isomers. The peak at 17.8 min has absorption maxima at 247, 315, and 363 nm.

The methanol fractions (Fig. S3D) also contained naphthoquinones of interest, but these fractions exhibited greater chemical complexity. This effect was expected as polar substances can be solubilized in organic solvents with these characteristics due to the polar, acidic, and basic character of the solvent (Nam et al. 2015).

The subfraction S1 (Fig. S3E) presented maximum absorption peak (18.9 min) suggestive of naphthalene, previously discussed. The subfraction S2 (Fig. S3F) presented peaks at 16.8 and 17.2 min in the dichloromethane, ethyl acetate, and methanol fractions showed absorption maxima at 247 and 268 nm, suggestive of 1,4-naphthoquinone compounds. Naphthoquinones with ketone substitutions at positions 1 and 4 have maximal ultraviolet absorption at ~250 nm (lawsone and plumbagin), which is characteristic of this class (Rodrigues et al. 2006). Another characteristic of naphthoquinones is their visible color ranging from yellow spots to shades of red. Here, both the ethanol extract and the fractions, when analyzed on TLC, presented yellow bands which is characteristic of this class of secondary metabolites.

Earlier studies have described the isolation of eleutherin and isoleutherin naphthoquinones as well as that of eleutherol, which belongs to the class of naphthalene (Paramapojn et al. 2008). To obtain the abovementioned naphthoquinones, the dichloromethane fraction of *E. plicata* was fractionated via solid–liquid chromatography. After successive purifications, three compounds were isolated, whose chromophores were used to identify eleutherol (Fig. S3E), eleutherin, and isoleutherin.

Eleutherol (RT = 18.9 min) was identified by co-injection with an eleutherol standard. Eleutherin (Table S1) and isoeleutherin (Table S2) were identified via NMR ^1H and the obtained spectra were compared with the literature data.

Antiplasmodial activity

In the microtest assay, the ethanol extract exhibited an IC_{50} of 55.65 ± 9.34 µg/mL, dichloromethane fraction (81.94 ± 32.09 µg/mL), and methanol fraction (89.91 ± 29.67 µg/mL) were classified as poorly active. Ethyl acetate (10.22 ± 2.32 µg/mL), eleutherin (10.45 ± 3.13 µg/mL), isoeleutherin (8.70 ± 2.45 µg/mL), and S2 fraction (eleutherin + isoeleutherin: 3.67 ± 1.01 µg/mL) were classified as active. However, the methanol fraction and S1 fraction (eleutherol) were inactive, exhibiting IC_{50} values of >200 µg/mL. Chloroquine was used as a positive control (Table 1).

Table 1 IC_{50} values of the *E. plicata* against chloroquine sensitive *P. falciparum* stain 3D7

Samples	IC_{50} μg/mL ± DP	Classification
EEEP	55.65 ± 9.34	Moderately active
FrDCM EP	81.94 ± 32.08	Moderately active
FrAcOET EP	10.22 ± 2.38	Active
FrMeOH EP	89.91 ± 29.67	Moderately active
Fr S1 (eleutherol)	>200	Inactive
Fr S2(eleutherin + isoeleutherin)	3.67 ± 1.01	Active
Isoeleutherin	8.70 ± 2.45	Active
Eleutherin	10.45 ± 3.13	Active
Chloroquine	0.023 ± 0.009	Very active

EEEP ethanol extract of *E. plicata*, *FrDCM EP* dichloromethane fraction of *E. plicata*, *FrAcOEt* ethyl acetate fraction of *E. plicata*, *FrMeOH EP* methanol fraction the *E. plicata*, *Fr S1* eleutherol, *Fr S2* eleutherin and isoeleutherin mixture, *NR* not performed, *SD* standard deviation

Dolabela et al. (2015b) demonstrated that the ethanol extract of *E. plicata* bulbs (6.57 μg/mL) and its dichloromethane fraction (2.87 μg/mL) were active against chloroquine resistant *P. falciparum* clone (W2) (Dolabela et al. 2015a). The results indicate that the naphthoquinones eleutherin and isoeleutherin are responsible for antiplasmodial activity, since the lowest IC_{50} values were obtained from the samples that have these compounds in greater quantity. When comparing the IC_{50} values obtained here with those reported by Dolabela et al. (2015b), these samples showed greater activity towards the chloroquine resistant stain.

Naphthoquinones are widely reported in the literature due to their antimalarial activity (López et al. 2014; Imperatore et al. 2019). Lapachol, a para-naphthoquinone, and similar compounds have been screened against chloroquine resistant *P. falciparum* (W2) strains. Lapachol exhibited an IC_{50} of 80.4 μM, but its methylated derivative (IC_{50} 15.8 μM) and that acetylated at hydroxyl position 2 (IC_{50} 2.3 μM) were more active, which was related to inefficient hemozoin formation by the parasite. Lapachol isomers, alpha-lapachone (IC_{50} 15.8 μM) and its methylated structure (IC_{50} 19.4 μM) as well as beta-lapachone (IC_{50} 20.5 μM) and another methylated derivative (IC_{50} 15.8 μM), were less promising than acetylated lapachol (Moreira et al. 2015). Thus, it was suggested that the orientation of the para-positioned naphthoquinone ketones contributes to the antimalarial activity. This hypothesis is further reinforced by atovaquone, which is a well-known para-naphthoquinone and a potent antimalarial drug whose mechanism of action involves the inhibition of ubiquinone oxireduction at the mitochondrial cytochrome bc_1 complex site (Vaidya and Mather 2009).

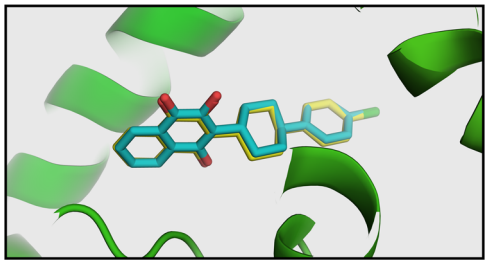

Fig. 2 The structure obtained by redocking (blue), overlapping the crystallographic structure (yellow) of atovaquone-bound complex

Molecular binding analysis

The three-dimensional structure of cyt bc_1 protein was obtained from the protein data bank (PDB ID: 4PD4) (Birth et al. 2014a). Previous study demonstrated high homology between the protein of the *S. cerevisiae* and the *P. falciparum*, with conservation of amino acid residues (Phe129, Met139, Trp142, Gly143, Val146, Ile147, Ile269, Pro271, Tyr279, Leu282) present at the atovaquone binding site (Birth et al. 2014a). Because there was no crystallography of the cyt bc_1 of *P. falciparum* mitochondrial, the protein of the *S. cerevisiae*.

Atovaquone, another naphthoquinone, binds to Plasmodium's mitochondrial cyt bc_1 complex. Since isoleuterine and eleuterine belong to the same chemical class, the same molecular target was selected for docking (Kessl et al. 2003; Birth et al. 2014a, 2014b; Siregar et al. 2015).

To validate the developed methodology, the position of the atovaquone crystallographic ligand was reproduced in silico in the binding pocket of cyt bc_1. Thus, atovaquone was re-docked at the protein binding site using the Molegro Virtual Docking 5.5 docking feature.

To evaluate the conformations observed upon redocking, RMSD values were considered. The RMSD value for atovaquone showed a small deviation (1.05 Å), where the mode of connection obtained in silico is very close to the experimentally determined values from crystallographic studies. This demonstrates that the docking protocol is capable of generate binding conformations capable of predicting the experimentally observed mode of interaction (Fig. 2). This molecular docking approach has been successfully used to investigate the interaction of naturally occurring compounds with various receptors (Neves Cruz et al. 2019b; Ramos et al. 2019).

After validating the docking protocol, the interaction mode of eleutherin and isoleutherin with cyt bc_1 was investigated. The overlap of eleutherin and isoleutherin binding modes can be seen in Fig. S4. These molecules showed MolDock Score values similar to those obtained for the atovaquone positive control (MolDock score = −89.05 kcal/mol). The MolDock scores for eleutherin and isoleutherin were −80.17 and

−83.21 kcal/mol, respectively (Table 2), indicating that ligands interacted favorably with the protein.

To further understand the binding mode of eleutherin and isoeleutherin, structural analyses were performed to identify the interactions between the compounds and amino acids of the cyt bc_1 binding cavity. In this manner, the interactions established between atovaquone and cyt bc_1 were identified (Fig. 3 and Table S3).

The antimalarial drug atovaquone showed pi–alkyl interactions with the following amino acids: Val146, Gly143, Met139, Ile269, Pro271, and Phe296 (Fig. 3a). In addition, π–π interactions were established between the amino acid side chain phenol of Tyr279 and the inhibitor head group. Two additional alkyl-like interactions were formed between the ligand and Leu275 and Ile299.

Eleutherin established hydrophobic pi–alkyl interactions with Met139, Ile269, Pro271, Phe129, and Tyr279 (Fig. 3b). An amide–pi interaction was established with Trp142 and two hydrophobic alkyl interactions were formed with Ile147 and Leu275. The Glu272 carboxyl formed a hydrogen bond with the inhibitor. Isoeleutherin established pi–alkyl interactions with Met139, Val146, Ile269, and Pro271, as well as an amide–pi hydrophobic interaction with Trp142 (Fig. 3c).

Table 2 Docking results obtained by the MolDock score

Ligand	MolDock score (kcal/mol)
Atovaquone	−89.05
Eleutherin	−80.17
Isoeleutherin	−83.21

Naphthoquinones, unlike atovaquone, do not contain long side chains, often referred to as a tail, attached to the core formed by the three rings, referred to as the head group. These compounds interacted with the binding pocket portion occupied by the head group of the atovaquone. Although the analyzed molecules exhibited a larger molecular volume than the atovaquone head group, it did not interfere with binding pocket accommodation and allowed interactions with several amino acids in the active site.

Birth et al. (2014a, 2014b) observed that the head group of the atovaquone is capable of forming interactions with cyt bc_1 amino acids from *S. cerevisiae* which presents high homology to *P. malariae, P. ovale, P. knowlesi, P. vivax*, and *P. falciparum* in their crystallography studies (Birth et al. 2014a). Eleutherin and isoleutherin established highly conserved amino acid interactions in the abovementioned Plasmodium species (Ile269, Gly143, Met139, Pro271, His181, Tyr279, and Val146).

The interactions with these residues were hydrophobic in the complexes established by eleutherin and isoleutherin, occurring mainly with the head groups. This indicates that these compounds can be active against different species (*P. malariae*, *P. ovale*, *P. knowlesi*, *P. vivax*, and *P. falciparum*) because the binding cavity of cyt bc_1 is highly conserved.

Conclusions

Ethanol extract of *E. plicata*, your dichloromethane, and ethyl acetate fractions showed antipalsmodial activity, this

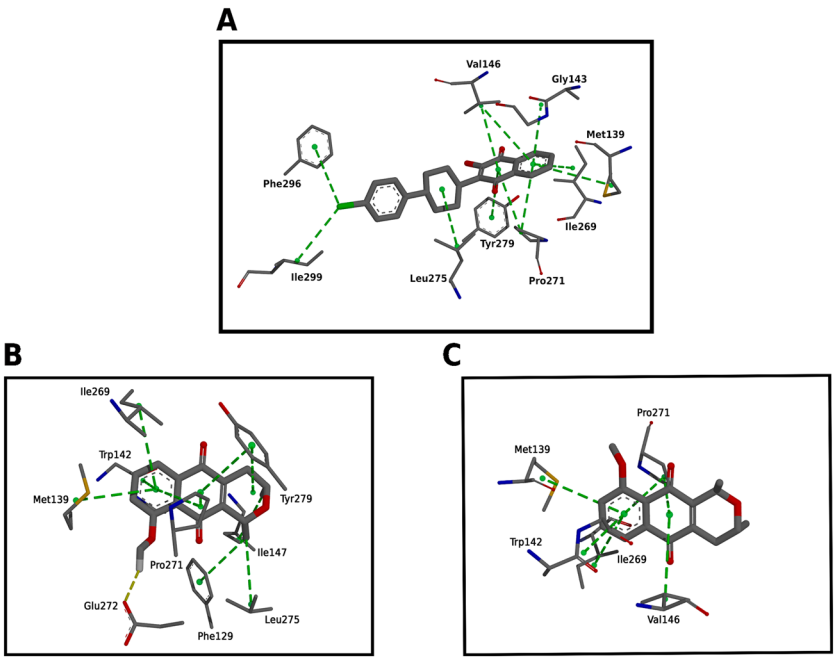

Fig. 3 Binding mode of (**a**) atovaquone, (**b**) eleutherin, and (**c**) isoeleutherin in the binding cavity of cyt bc_1. Carbon atoms are represented in gray, nitrogen in blue, oxygen in red, sulfur in yellow, and hydrogen in white. Hydrophobic interactions are represented by green dashed lines and hydrogen bonds are represented by yellow dashed lines

activity is related to isoeleutherin (IC_{50} 8.70 ± 2.45 μg/mL) and eleutherin (IC_{50} 10.45 ± 3.13 μg/mL). Through in silico analysis compounds interacted with highly conserved cytochrome bc1 residues, establishing hydrophobic interactions and hydrogen bonds. Thus, this study demonstrated that isoleutherin and eleutherin are promising candidates as novel antimalarial drugs capable of causing mitochondrial damage to the parasite.

Acknowledgements This study was financed in part by the Coordination of Superior Level Staff Improvement (CAPES) and National Council for Scientific and Technological Development (CNPq).

Compliance with ethical standards

Conflict of interest The authors declare that they have no conflict of interest.

Publisher's note Springer Nature remains neutral with regard to jurisdictional claims in published maps and institutional affiliations.

References

Alves TMA, Kloos H, Zani CL (2003) Eleutherinone, a novel fungitoxic naphthoquinone from Eleutherine bulbosa (Iridaceae). Mem Inst Oswaldo Cruz. https://doi.org/10.1590/S0074-02762003000500021

Alves FS, de AR do Rego J, da Costa ML et al. (2019) Spectroscopic methods and in silico analyses using density functional theory to characterize and identify piperine alkaloid crystals isolated from pepper (Piper nigrum L.). J Biomol Struct Dyn. https://doi.org/10.1080/07391102.2019.1639547

Becke AD (1993) Density-functional thermochemistry. III. The role of exact exchange. J Chem Phys. 98:5648–5652. https://doi.org/10.1063/1.464913

Birth D, Kao W-C, Hunte C (2014a) Structural analysis of atovaquone-inhibited cytochrome bc1 complex reveals the molecular basis of antimalarial drug action. Nat Commun 5:4029. https://doi.org/10.1038/ncomms5029

Birth D, Kao W, Hunte C (2014b) Structural analysis of mitochondrial cytochrome bc1 complex with atovaquone bound reveals the molecular basis of antimalarial drug action. Malar J 13: https://doi.org/10.1186/1475-2875-13-s1-p103

Lambros C, Vanderberg JP (1979) Synchronization of Plasmodium falciparum erythrocytic stages in culture. J Parasitol 65:418–420

Carvalho LH, Krettli AU (1991) Antimalarial chemotherapy with natural products and chemically defined molecules. Mem Inst Oswaldo Cruz. https://doi.org/10.1590/S0074-02761991000600041

Couto CLL, Moraes DFC, Cartágenes M, do SS et al. (2016) Eleutherine bulbous (Mill.) Urb.: a review study. J Med Plants Res. 10:286–297. https://doi.org/10.5897/JMPR2016.6106

Cowman AF, Healer J, Marapana D, Marsh K (2016) Malaria: biology and disease. Cell 167:610–624

da Costa KS, Galúcio JM, da Costa CHS, et al. (2019) Exploring the potentiality of natural products from essential oils as inhibitors of odorant-binding proteins: a structure- and ligand-based virtual screening approach to find novel mosquito repellents. ACS Omega acsomega. 9b03157. https://doi.org/10.1021/acsomega.9b03157

Das S, Tripathy S, Chattopadhayay S et al. (2017) Progressive increase in point mutations associates chloroquine resistance: even after withdrawal of chloroquine use in India. Int J Parasitol Drugs drug Resist 7:251–261. https://doi.org/10.1016/j.ijpddr.2017.06.002

Dennington R, Keith TA, Millam JM (2016) GaussView Version 6 Semichem Inc., Shawnee Mission, KS

Dolabela MF, Martins MT, Brandao DLDN et al. (2015a) Method for producing a plant extract and fraction, pharmaceutical compositions and use there of, United States, Patent Application Publication, Pub. No.: US 2015/0132421 A1, Pub. Date: 14 May 2015

Dolabela MF, Póvoa MM, Brandão GC, et al. (2015b) Aspidosperma species as sources of anti-malarials: uleine is the major antimalarial indole alkaloid from Aspidosperma parvifolium (Apocynaceae). Malar J. https://doi.org/10.1186/s12936-015-0997-4

Frisch MJ, Trucks GW, Schlegel HB, et al. (2016) Gaussian 16, Revision B.01. Gaussian, Inc., Wallingford, CT

Gallo FR, Palazzino G, Federici E et al. (2010) Polyketides from Eleutherine bulbosa. Nat Prod Res. 24:1578–1586. https://doi.org/10.1080/14786419.2010.500007

Geleta G, Ketema T (2016) Severe malaria associated with Plasmodium falciparum and P. vivax among children in Pawe Hospital, Northwest Ethiopia. Malar Res Treat 2016:1–7. https://doi.org/10.1155/2016/1240962

Hara H, Maruyama N, Yamashita S, et al. (2011) Elecanacin, a novel new naphthoquinone from the bulb of Eleutherine americana. Chem Pharm Bull. https://doi.org/10.1248/cpb.45.1714

Hong J-H, Yu ES, Han A-R et al. (2008) Isoeleutherin and eleutherinol, naturally occurring selective modulators of Th cell-mediated immune responses. Biochem Biophys Res Commun 371:278–282. https://doi.org/10.1016/j.bbrc.2008.04.060

Imperatore C, Persico M, Senese M et al. (2019) Exploring the antimalarial potential of the methoxy-thiazinoquinone scaffold: Identification of a new lead candidate. Bioorg Chem. 85:240–252. https://doi.org/10.1016/j.bioorg.2018.12.031

Junior M, Leite F, Santos C, et al. (2019) In silico study to identify new antituberculosis molecules from natural sources by hierarchical virtual screening and molecular dynamics simulations. Pharmaceuticals. https://doi.org/10.3390/PH12010036

Kessl JJ, Lange BB, Merbitz-Zahradnik T et al. (2003) Molecular basis for atovaquone binding to the cytochrome bc1 complex. J Biol Chem. 278:31312–31318. https://doi.org/10.1074/jbc.M304042200

Klotz LO, Hou X, Jacob C (2014) 1,4-naphthoquinones: from oxidative damage to cellular and inter-cellular signaling. Molecules. https://doi.org/10.3390/molecules190914902

Kusuma IW, Arung ET, Rosamah E et al. (2010) Antidermatophyte and antimelanogenesis compound from Eleutherine americana grown in Indonesia. J Nat Med. 64:223–226. https://doi.org/10.1007/s11418-010-0396-7

López LIL, Flores SDN, Belmares SYS, Galindo AS (2014) Naphthoquinones: biological properties and synthesis of lawsone and derivatives - a structured review. VITAE 21:248–258

Moreira DRM, De Sá MS, Macedo TS et al. (2015) Evaluation of naphthoquinones identified the acetylated isolapachol as a potent and selective antiplasmodium agent. J Enzyme Inhib Med Chem. https://doi.org/10.3109/14756366.2014.958083

Nam MW, Zhao J, Lee MS et al. (2015) Enhanced extraction of bioactive natural products using tailor-made deep eutectic solvents: application to flavonoid extraction from Flos sophorae. Green Chem. https://doi.org/10.1039/c4gc01556h

Neves Cruz J, da Costa KS, de Carvalho TAA, de Alencar NAN (2019a) Measuring the structural impact of mutations on cytochrome P450 21A2, the major steroid 21-hydroxylase related to congenital adrenal hyperplasia. J Biomol Struct Dyn. https://doi.org/10.1080/07391102.2019.1607560

Neves Cruz J, Oliveira M, Gomes Silva S et al. (2019b) Insight into the interaction mechanism of nicotine, NNK and NNN with cytochrome P450 2A13 based on molecular dynamics simulation. J Chem Inf Model ACS 9b00741. https://doi.org/10.1021/acs.jcim.9b00741

Newman DJ, Cragg GM (2016) Natural products as sources of new drugs from 1981 to 2014. J Nat Prod 79:629–661

Paramapojn S, Ganzera M, Gritsanapan W, Stuppner H (2008) Analysis of naphthoquinone derivatives in the Asian medicinal plant Eleutherine americana by RP-HPLC and LC-MS. J Pharm Biomed Anal 47:990–993. https://doi.org/10.1016/j.jpba.2008.04.005

Phillips MA, Burrows JN, Manyando C et al. (2017) Malaria. Nat Rev Dis Prim 3: https://doi.org/10.1038/nrdp.2017.50

Rahmatullah M, Rahman T, Jahan R (2012) Anti-malarial plants used in folk medicine in Bangladesh. In: M. K. Rai, Geoffrey A. Cordell, Jose L. Martinez, Mariela Marinoff LR (eds) Medicinal Plants: Biodiversity and Drugs, 1st edn. CRC Press, pp 241–290

Ramos RS, Macêdo WJC, Costa JS et al. (2019) Potential inhibitors of the enzyme acetylcholinesterase and juvenile hormone with insecticidal activity: study of the binding mode via docking and molecular dynamics simulations. J Biomol Struct Dyn 1–31. https://doi.org/10.1080/07391102.2019.1688192

René Thomsen MHC, Thomsen R, Christensen MH (2006) MolDock: a new technique for high-accuracy molecular docking. J Med Chem. 49:3315–3321. https://doi.org/10.1021/jm051197e

Rieckmann KH, Campbell GH, Sax LJ, Mrema JE (1978) Drug sensitivity of Plasmodium falciparum. an in-vitro microtechnique. Lancet 1:22–23. https://doi.org/10.1016/s0140-6736(78)90365-3

Rodrigues SV, Viana LM, Baumann W (2006) UV/Vis spectra and solubility of some naphthoquinones, and the extraction behavior of plumbagin from Plumbago scandens roots in supercritical CO2. Anal Bioanal Chem. 385:895–900. https://doi.org/10.1007/s00216-006-0502-6

Siciliano G, Alano P (2015) Enlightening the malaria parasite life cycle: Bioluminescent Plasmodium in fundamental and applied research. Front Microbiol 6:1–8. https://doi.org/10.3389/fmicb.2015.00391

Singh B, Daneshvar C (2013) Human infections and detection of Plasmodium knowlesi. Clin Microbiol Rev 5: https://doi.org/10.1128/CMR.00079-12

Siregar JE, Kurisu G, Kobayashi T et al. (2015) Direct evidence for the atovaquone action on the Plasmodium cytochrome bc1 complex. Parasitol Int. 64:295–300. https://doi.org/10.1016/j.parint.2014.09.011

Talapko Škrlec, Alebić et al. (2019) Malaria: the past and the present. Microorganisms 7:179. https://doi.org/10.3390/microorganisms7060179

Tewierik LM, Dimitriadis C, Donner CD et al. (2006) Total synthesis of enantiopure 1,3-dimethylpyranonaphthoquinones including ventiloquinones E, G, L and eleutherin. Org Biomol Chem. 4:3311–3318. https://doi.org/10.1039/b607366b

Vaidya AB, Mather MW (2009) Mitochondrial evolution and functions in malaria parasites. Annu Rev Microbiol 63:249–267. https://doi.org/10.1146/annurev.micro.091208.073424

Wang Z, Shrestha S, Li X et al. (2015) Prevalence of K13-propeller polymorphisms in Plasmodium falciparum from China-Myanmar border in 2007-2012. Malar J. 14:168. https://doi.org/10.1186/s12936-015-0672-9

WHO (2018) World Malaria Report. World Health Organization, Geneva